Surface Science 603 (2009) 2387–2392

Contents lists available at ScienceDirect

Surface Science

journal homepage: www.elsevier.com/locate/susc

Ab-initio calculations of interactions between Cu adatoms on Cu(1 1 0): Sensitivity of strong multi-site interactions to adatom relaxations

Rajesh Sathiyanarayanan *, T.L. Einstein

Department of Physics, University of Maryland, College Park, MD 20742-4111, USA

ARTICLE INFO

Article history:
Received 7 April 2009
Accepted for publication 21 May 2009
Available online 6 June 2009

Keywords:
Density-functional calculations
Low-index single crystal surfaces
Lattice–gas models
Copper
Adatom relaxations
Surface diffusion

ABSTRACT

We have parameterized the various interactions between Cu adatoms on Cu(1 1 0) using density-functional theory based ab-initio calculations. Our results indicate that in addition to pair interactions, 3-adatom and 4-adatom interactions of significant strengths are present in this system. This further stresses the importance of multi-site interactions in constructing a complete lattice–gas picture. Even though adding these multi-site interactions leads to good convergence in interaction energies, we find that some multi-site interactions are very sensitive to adatom relaxations. This makes the application of a simple lattice–gas picture inadequate for such surfaces. We also parameterize adatom interactions on this surface using the recently developed connector model. The connector model parameterization is as efficient as the parameterization using lattice–gas model. Further, we present diffusion barriers for nearest-neighbor (NN) and next-nearest-neighbor (NNN) hops on this surface.

1. Introduction

A thorough understanding and characterization of surface energetics is important for fabricating nanostructures with desired morphological features. To this end, lattice–gas models have been very successful in characterizing interactions between adatoms on a surface [1–4]. The general idea being that a set of interactions is sufficient to understand both equilibrium and dynamic surface processes. With advances in computational power and the development of density-functional theory (DFT) based software packages such as VASP (Vienna Ab-initio Simulation Package) [5–8], these interactions can now be computed with reliable accuracy.

The basic assumptions that underlie lattice–gas models are: (i) all atoms sit at high-symmetry positions and local relaxations produce the final structure, (ii) a finite set of effective interactions is sufficient to understand all the surface processes and (iii) interactions are not sensitive to local positions of the adatoms. In the simplest scenario, only pair interactions between nearest neighbors are considered. However, in certain cases, like the orientation dependence of step stiffness and the equilibrium shape of islands, long-range pair interactions and multi-site interactions are required for a complete description [9–17]. Multi-site interactions often have a large elastic component; hence, a careful consideration of surface relaxation effects is needed while computing them.[1] We have shown that multi-site interactions, trios in particular, are very sensitive to lateral relaxation of adatoms on Cu(1 0 0) and Pt(1 1 1) and hence the application of a simple lattice–gas picture in those cases leads to erroneous results [16].

Experimental studies of Al(1 1 0) homoepitaxy have reported the formation of regular pyramidal islands (nanohuts) under certain growth conditions [18]. Using DFT calculations, Zhu et al. computed the relevant diffusion barriers for understanding the mechanism behind the formation of such nanohuts [19]. Further, mechanisms for upward self-diffusion of individual adatoms and small adatom clusters have also been found to exist on Al(1 1 0) and Cu(1 1 0) surfaces and the formation of nanohuts is predicted on Cu(1 1 0) and other fcc metal (1 1 0) surfaces [20]. As a substrate, Cu(1 1 0) finds application in the molecular self-assembly of a large number of aromatic compounds; particularly in the case of a benzoate molecule, the presence of Cu adatoms influences the orientation of the molecular assembly [21]. Ever since high magnetoresistance was found on Co/Cu [22] multilayers, Co thin-film growth on Cu surfaces has generated much interest among surface scientists due to potential applications in the field of spintronics. All of these findings make the first-principles based study of surface energetics and thin-film growth on Cu(1 1 0) technologically important. Using VASP, we have characterized the interactions of Cu adatoms on Cu(1 1 0) and computed the diffusion barriers for

* Corresponding author. Fax: +1 301 3149465.
E-mail addresses: srajesh@umd.edu (R. Sathiyanarayanan), einstein@umd.edu (T.L. Einstein).

[1] Surface relaxation effects are especially important for multi-site interactions between closely spaced adatoms because of significant contributions from direct interactions between them.

0039-6028/$ - see front matter © 2009 Elsevier B.V. All rights reserved.
doi:10.1016/j.susc.2009.05.012

NN (nearest-neighbor) and NNN (next-nearest-neighbor) for the same system.

In contrast to adatom interactions on Al(1 1 0), we find that the strongest pair and multi-site interactions are attractive. We also find that certain trio and quarto interactions have strengths comparable to pair interactions. Thus, such interactions are important in the lattice–gas picture. We discuss some of the problems associated with computing such interactions. These issues severely reduce the power of a lattice–gas based approach in studying surface processes. We also characterized the adatom interactions using the connector model [17], which was recently developed as an alternative approach to deal with the presence of many sizable multi-site interactions in a tractable way. We find the connector model is as efficient as the traditional lattice–gas model in parameterizing adatom interactions on this surface. In the light of this and similar results on Al [17], the connector model offers a feasible alternative for characterizing adatom interactions on (1 1 0) surfaces.

2. Computational details

To compute the interactions between Cu adatoms on Cu(1 1 0), we used density-functional theory [23,24] based VASP along with ultrasoft pseudopotentials and the Perdew-Wang '91 generalized gradient approximation (GGA)[2] [25]. We used an energy cut-off of 17.2 Ry for the plane-wave basis set and, to speed up the calculations, a Methfessel-Paxton [26] width of 0.2 eV. We used a lattice parameter of 3.64 Å determined from a bulk calculation with a $(1 \times 1 \times 1)$ supercell sampled with an $(11 \times 11 \times 11)$ k-point mesh. To check for consistency in the computed energy values, we computed the energies using two supercells with different lateral dimensions – $(4 \times 4 \times 16)$ and $(5 \times 4 \times 16)$ along $([1\,\bar{1}\,0] \times [0\,0\,1] \times z)$ sampled by $(4 \times 3 \times 2)$ and $(3 \times 3 \times 2)$ k-point meshes, respectively. Our slab was six atomic layers thick, and the rest of the supercell was filled with vacuum. In Table 1, we list the changes in interlayer separations for a plain slab (without any adatoms), computed using a $(4 \times 3 \times 16)$ supercell sampled by a $(4 \times 4 \times 2)$ k-point mesh, as a percentage of their bulk separations. The values are in good agreement with previous experimental measurements and theoretical calculations [27]. Since the change in interlayer separation between the third and fourth layers is very small (less than 1%, approximately 0.01 Å), we allowed only the top three layers to relax. We put adatoms on only one side of the slab to avoid adatom interactions through the slab because the interlayer spacing for layers on a (1 1 0) surface is smaller than on (1 0 0) or (1 1 1) surfaces. Placing adatoms on only side facilitates the usage of slabs of computationally feasible thickness for surface energy calculations. Since charge transfer effects are not expected to be significant for this case, this asymmetry should not have any significant effect. All atoms were allowed to relax till the forces on them were less than 0.01 eV/Å.

We used the leave-n_v-out cross-validation method [28] to fit the computed energies to the interaction parameters. This method is expected to perform better than the commonly used leave-1-out cross-validation scheme [28]. The interaction strengths were calculated in the following way: for a particular supercell, total energies were computed for, say, n different configurations of adatoms. In addition to that, we posit the number of significant interactions (n_i). We then use n_i (out of n) equations to solve for the interaction energies. These interactions are then used to predict the energies of the remaining n_v ($n_v = n - n_i$) equations. The prediction error per adatom for a particular configuration j ($1 \leqslant j \leqslant n_v$) is calculated using the following equation

$$\Delta E_j = \frac{E^{pred}(j) - E^{\mathrm{VASP}}(j)}{a_j} \tag{1}$$

where a_j denotes the number of adatoms in that configuration. The root mean squared (rms) value of those errors

$$\Delta E_{\mathrm{rms}} = \sqrt{\frac{1}{n_v}\sum_{j=1}^{n_v}(\Delta E_j)^2} \tag{2}$$

is then calculated. This procedure is repeated for different partitions of (n, n_i), and sets of interactions from only those partitions whose ΔE_{rms} values are lower than a certain threshold value (10 meV/adatom) are considered for the final averaging of interaction values. The number of significant interactions is varied, and the one with the best convergence ($n_i = 9$ for lattice–gas model and $n_i = 10$ for connector model) is found. This procedure is repeated for both supercells. To test for consistency, we also present cross-validation (CV) scores (rms value of per adatom prediction errors) obtained when interaction energies computed for a particular supercell, say $(4 \times 4 \times 16)$, are used to predict energies of adatom clusters in $(5 \times 4 \times 16)$ supercell.

Table 1
Change in the interlayer separation between i and $i+1$ layers expressed as a percentage of the corresponding bulk value. The values were calculated using a $(3 \times 4 \times 16)$ supercell with a slab that is 10 atomic layers thick. Only the top five layers were allowed to relax; the rest of the layers were fixed at their bulk positions. The error bars inside the parentheses give the range of variation of these values for different supercells and different number of relaxing layers.

$(i, i+1)$	$\Delta d_{i,i+1}$ (%)
(1, 2)	−9.7 (±0.6)
(2, 3)	+4.0 (±0.8)
(3, 4)	−1.9 (±0.3)
(4, 5)	+0.4 (±0.4)
(5, 6)	+0.08

3. Results and discussion

The lattice–gas interactions of adatoms calculated using two different supercells are listed in Table 2. We considered six pair interactions with a maximum range of 7.28 Å (twice the lattice spacing), four trio interactions and three quarto interactions. Except fifth-neighbor and sixth-neighbor interactions, all interactions that were considered are shown in Fig. 1. The pair interactions E_5 and E_6 were found to be very weak (around 5 meV) and including them worsened the CV scores. Three of the multi-site interactions, E_{T2}, E_{Q2} and E_{Q3}, were not found to be significant. This makes the presence of sizable five-adatom quinto interactions on this surface improbable; accordingly, we exclude them. Since E_{Q3} is small, presence of a strong collinear quinto is unlikely. Also the two quintos that can be formed by adding an adatom either along the in-channel or along the cross-channel direction to the only sizable quarto interaction, E_{Q1}, can be reasonably neglected due to the smallness of E_{Q2} and E_{C2} interactions.

The interaction energies computed using the two supercells are in very good agreement with each other. The CV scores are very low (at most 9 meV/adatom) and the maximum CV error for any case is only 23 meV/adatom (approximately $1k_BT$ at room temperature). As expected, the first-neighbor attraction is the strongest interaction on the surface. Surprisingly, the next strongest interaction is the collinear trio interaction, E_{C1}. The strong attractive nature of both interactions explain the formation of long 1D islands at low temperatures ($T < 220$ K) along the in-channel direction as

[2] Our tactic here is to employ the best available purely-theoretical method, which in turn is now routinely used to fit parameterized potentials. We do not address the question of whether a purely-theoretical approach describes actual potential surfaces more accurately than a sophisticated many-parameter semiempirical (i.e. fit to experimental data rather than theoretical data) approach.

Table 2
Lattice–gas energies of Cu adatoms on Cu(1 1 0) computed using (4 × 4 × 16) and (5 × 4 × 16) supercells with total, *z*- and no-relaxation schemes. All energies are given in meV and the CV values are given in meV/adatom. The numbers inside the parentheses indicate the absolute value of maximum CV error.

Interactions	Total relaxation		*z*-relaxation		No-relaxation	
	(4 × 4 × 16)	(5 × 4 × 16)	(4 × 4 × 16)	(5 × 4 × 16)	(4 × 4 × 16)	(5 × 4 × 16)
E_0	−3536	−3534	−3535	−3529	−3520	−3513
E_1	−223	−235	−209	−215	−230	−246
E_2	−31	−29	−35	−36	−33	−30
E_3	+5	+5	−19	−5	−7	+5
E_4	+13	0	+21	0	+19	0
E_{C1}	−60	−45	−68	−57	−71	−54
E_{C2}	−5	−10	−3	−7	−2	−6
E_{T1}	+16	+17	+20	+16	+7	+3
E_Q	−30	−19	−16	−6	+24	+32
CV (4 × 4 × 16)	4 (14)	9 (23)	2 (3)	9 (19)	2 (4)	9 (19)
CV (5 × 4 × 16)	3 (6)	2 (4)	5 (13)	2 (4)	6 (13)	2 (4)

seen by Mottet et al. in their kinetic Monte Carlo simulations [29]. Also, the computed values of E_1 and E_2 are in good agreement with their values. The other pair interactions, E_3 and E_4, are small and repulsive. Remarkably, of the five strongest interactions, three are multi-site interactions. Recently, such multi-site interactions have been found on a variety of metallic surfaces [9–17]. Thus, multi-site interactions become vital for constructing a complete lattice–gas picture [30]. However, there are certain difficulties involved in computing such multi-site interactions accurately. Such issues are discussed in Section 3.1. Also there is a discrepancy in the value of E_4 computed between the two supercells. This raises an interesting issue and is dealt with in detail in Section 3.2. Results from parameterizing adatom interactions using the connector model are given in Section 3.3, and diffusion barriers for hopping to neighbor sites are given in Section 3.4.

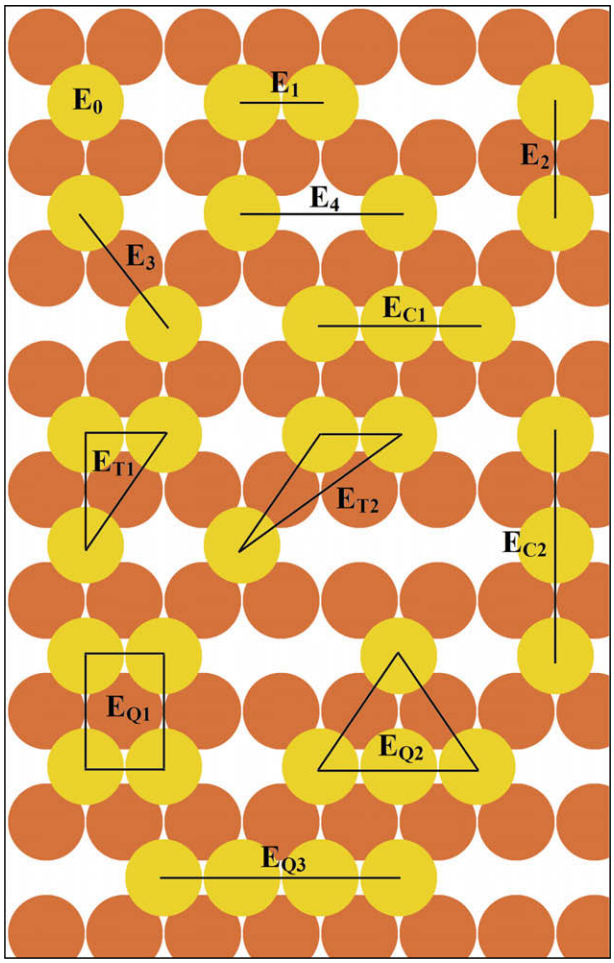

Fig. 1. Lattice–gas interactions used to characterize Cu adatom interactions on Cu(1 1 0). In all the figures, lighter mustard circles represent adatoms and darker orange circles represent atoms in the substrate layer. Multi-site interactions, E_{T2}, E_{Q2} and E_{Q3}, were found to be insignificant. Table 2 gives the values of these interaction energies for different relaxation schemes. (For interpretation of the references to colour in this figure legend, the reader is referred to the web version of this article.)

3.1. Adatom relaxations and multi-site interactions

When adatoms were allowed to relax along all directions, the displacements were found to be primarily along the *z*-direction. The percentage changes in atomic separations along the three directions due to relaxations are listed in Table 3. It is evident that the reductions (both percentage and absolute) in adatom separations along the *z*-direction are much greater than the corresponding values for the two lateral directions. To assess the effect of relaxation on the interaction energies, we computed interaction strengths with two different relaxation schemes – (i) *z*-relaxation: atoms are allowed to relax only in the vertical direction and lateral relaxations are suppressed and (ii) no-relaxation: atoms are frozen in their bulk positions; atomic relaxations along all directions are suppressed. The interaction energies for the cases of *z*- and no-relaxations are also given in Table 2.

Comparing the energy values computed using total and *z*-relaxation schemes helps to identify the effects of lateral relaxations on lattice–gas energies. When adatom interactions are computed using the *z*-relaxation scheme, almost all interaction energies, except E_3 and E_{Q1}, are close to the corresponding values obtained with total relaxation. This could be attributed to the point mentioned above about the relative magnitudes of relaxations along the three directions. It is surprising that among the pair interactions, only E_3 changes due to the suppression of lateral relaxations. Since both the interaction and the corresponding change have small magnitudes, we cannot tell whether the change is due to elastic interactions or some unaccounted-for long-range interaction. On the other hand, the decrease in the magnitude of the rectangular quarto interaction, E_{Q1}, is readily explained: E_{Q1} arises from the suppression of lateral relaxations of the trios, E_{T1}, when such

Table 3
Percentage reduction in the distance between adatoms from the bulk value due to adatom relaxation. To get absolute reduction, the values should be scaled by $2a{:}2\sqrt{2}a{:}a$ where a = 3.64 Å is the lattice spacing.

Supercells	$\Delta d_{[1\,1\,0]}$ (%)	$\Delta d_{[0\,0\,1]}$ (%)	Δz%
(4 × 3 × 16)	−3.1	−1.3	−11.3
(4 × 4 × 16)	−3.0	−0.4	−11.0
(5 × 4 × 16)	−3.0	−0.3	−11.5

trios are found in the 2D-bulk layer of adatoms rather than near island edges. The same issue for Cu(1 0 0) is discussed in detail in our previous paper [16]. Since lateral relaxations are suppressed in the *z*-relaxation scheme, there is no difference in the values between the E_{T1} trios near the island edges and the ones in the 2D-bulk layer. Hence, the magnitude of E_{Q1} decreases significantly in the case of *z*-relaxation. The CV scores for *z*-relaxation are as low as the ones obtained in the case of total relaxation.

Most of the interaction energies computed using the no-relaxation scheme do not differ considerably from the ones computed using *z*-relaxation. The only interactions whose values change remarkably are E_{T1} and E_{Q1}. Compared with the corresponding values in the case of *z*-relaxation, E_{T1} decreases by more than half; from a moderately strong repulsion, it becomes vanishingly small. The change is even more drastic for values of E_{Q1}. From a strong attractive interaction (comparable in magnitude to E_2) in total relaxation scheme, E_{Q1} changes to a weak attraction when lateral relaxations are suppressed and, in turn, becomes a strong repulsive interaction in the case of no-relaxation. The difference between the *z*- and no-relaxation schemes is that in the latter, adatoms cannot optimize the lengths of their bonds with underlying substrate atoms. Therefore, it is reasonable that the corresponding changes in interaction values are drastic for those interactions (E_{T1} and E_{Q1}) that share a common substrate atom.[3] The cases of E_{T1} and E_{Q1} stress the importance of relaxation effects while computing the strengths of multi-site interactions.

On the other hand, the other two multi-site interactions, E_{C1} and E_{C2}, seem insensitive to relaxation effects. Their values do not undergo any significant change under different relaxation schemes. Previously [16] we gave the following argument for the higher sensitivity of multi-site interactions compared to pair interactions: *in pair interactions, owing to symmetry, lateral relaxations must occur along the bond direction. Since stretching or squeezing a bond is energetically expensive, the relative position of those adatoms does not change much, thereby making pair interactions less sensitive to relaxations*. By the same reasoning, the adatoms in E_{C1} and E_{C2} interactions, due to symmetry, are forced to relax either along the close-packed [1 $\bar{1}$ 0] or the [0 0 1] directions, the two primary bond directions on (1 1 0). As a result, the strengths of E_{C1} and E_{C2} interactions are unaffected by adatom relaxations. Also, among the pair interactions, only the E_3 adatom pair is not bound by symmetry to relax along any bond directions. This could explain its fluctuations with respect to relaxation schemes.

In summary, in the lattice–gas approach to overlayer systems, certain multi-site interactions, and probably pair interactions, are found to be very sensitive to adatom relaxations. The multi-site interactions that are very sensitive to adatom relaxations, E_{T1} and hence E_{Q1}, are the ones necessary to describe energies of adatoms near island edges. These are the interactions relevant for computing experimentally verifiable physical quantities like step stiffness and island shapes. Hence, a careful consideration of relaxation effects is important while computing the values of such interactions. Accounting for relaxation effects in surface energies calculations requires either the introduction of higher order multi-site interactions or the use of large supercells (to minimize frustrated relaxations). In addition to increasing the computational cost associated with the problem, such ad hoc approaches also severely undermine the fundamental soundness of lattice–gas models.

[3] In the *z*- relaxation scheme, among all the atoms in the substrate layer, the atom shared by the E_{Q1} quarto adatoms, due to the highest value of its coordination number, gets closest to the adatom layer. It is followed by the substrate atom shared by the E_{T1} trio due to the same reason. The change in the interlayer separation (measured along the *z*-direction) between the E_{Q1} quarto and the shared substrate atom is −14.7% and the corresponding change for E_{T1} trio and the shared substrate atom is −13.4%. In comparison, the change in the interlayer separation of a lone adatom and its nearest-neighbor substrate atom is −11.4%.

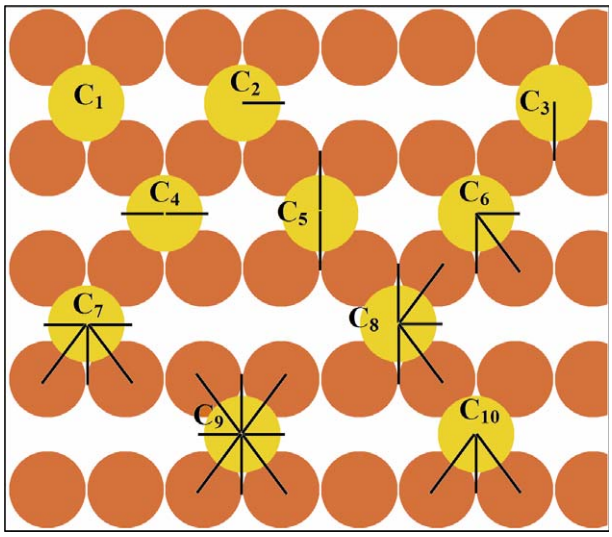

Fig. 2. Connectors [17] used to characterize Cu adatom interactions on Cu(1 1 0). Table 3 gives the values of these interactions for different relaxation schemes.

3.2. Multi-site interactions as corrections to pair interactions – discrepancy in E_4 values

In all relaxation schemes, there is a difference between E_4 values calculated using $(4 \times 4 \times 16)$ and $(5 \times 4 \times 16)$ supercells. The interaction E_4 is mildly repulsive in $(4 \times 4 \times 16)$ supercells, whereas it is negligible in $(5 \times 4 \times 16)$ supercells. This discrepancy can be understood if we consider E_4 values along with E_{C1} values in these two supercells. In the case of total relaxation, the difference in E_4 values is 13 meV with the $(4 \times 4 \times 16)$ value being higher. At the same time, their E_{C1} values differ[4] by −15 meV. The discrepancy between these two values is not surprising because the collinear trio interaction (E_{C1}) is, in fact, a correction term to fourth-neighbor (E_4) interaction due to the presence of an adatom between the atoms that make up the pair. Also in $(5 \times 4 \times 16)$ supercells, the numbers of E_4 interactions in all of our adatom configurations are either equal or very close to the corresponding numbers of E_{C1} interactions. Thus, the difference in E_4 is compensated by E_{C1} values such that the *sums* of those two interactions, calculated using the two supercells, are very close to each other. The difference[3] between $E_{C1} + E_4$ values is −2 meV for total relaxation and 10 meV and 2 meV in the cases of *z*- and no-relaxations. Such discrepancies might arise when multi-site interactions are used as corrections to pair interactions and also when multi-site interactions that form a non-compact cluster[5] of adatoms are used to parameterize adatom interactions. However, it does not pose a serious problem to the accuracy of the interaction energies in this case can be seen from the low CV scores.

3.3. Connector energies

In the connector model [17], each adatom in a cluster is mapped onto a particular connector that has the same number of each type of (first-, second-, and if necessary, third-) neighbor bonds.[6] The

[4] The energy difference (ΔE) is calculated as the energy value computed using $(5 \times 4 \times 16)$ supercells subtracted from the corresponding energy value computed using $(4 \times 4 \times 16)$ supercells.

[5] The quarto interaction, E_{Q2}, is a compact cluster but the same arrangement without the middle atom in the bottom row (middle atom in the collinear trio) is a non-compact or an open cluster.

[6] A more accurate model should also take into account the orientations of these bonds. However, doing so would increase the total number of connectors needed to parameterize the interactions, thereby reducing the efficacy of the model.

Table 4
Connector energies of Cu adatoms on Cu(1 1 0) computed using (4 × 4 × 16) and (5 × 4 × 16) supercells with total, *z*- and no-relaxation schemes. All energies are given in meV, and the CV values are given in meV/adatom. The numbers inside the parentheses indicate the absolute value of maximum CV error.

Connectors	Total relaxation		*z*-relaxation		No-relaxation	
	(4 × 4 × 16)	(5 × 4 × 16)	(4 × 4 × 16)	(5 × 4 × 16)	(4 × 4 × 16)	(5 × 4 × 16)
C_1	−3540	−3533	−3538	−3530	−3522	−3512
C_2	−3647	−3651	−3641	−3639	−3635	−3638
C_3	−3561	−3549	−3559	−3547	−3537	−3528
C_4	−3795	−3815	−3796	−3809	−3810	−3822
C_5	−3555	−3555	−3553	−3553	−3535	−3535
C_6	−3649	−3655	−3647	−3646	−3642	−3643
C_7	−3800	−3791	−3794	−3791	−3800	−3795
C_8	−3669	−3661	−3665	−3661	−3656	−3651
C_9	−3795	−3791	−3804	−3798	−3797	−3794
C_{10}	−3532	−3538	−3521	−3535	−3508	−3519
CV (4 × 4 × 16)	3 (7)	9 (25)	3 (8)	8 (21)	2 (5)	7 (17)
CV (5 × 4 × 16)	6 (13)	1 (3)	6 (12)	2 (7)	6 (11)	2 (5)

energy of the cluster is then written as the sum of the connector energies. One of the main features of this model is that the type of connector contains information about the local geometry of the adatom; hence relaxation effects are expected to be built into the model. We used 10 connectors (shown in Fig. 2) to characterize adatom interactions on Cu(1 1 0). Since E_3 is weak, an adatom was mapped to the connector with the same number of first-neighbor and second-neighbor bonds.[7]

Connector energies for all three relaxation schemes are listed in Table 4. The CV scores are as good as those obtained using the lattice–gas approach. This success is not surprising because each of the connector energies can be expressed as a linear combination of lattice–gas energies. For example, the connector C_6 can be written as

$$C_6 = E_0 + \frac{E_1}{2} + \frac{E_2}{2} + \frac{E_3}{2} + \frac{E_{T1}}{3} + \frac{E_{Q1}}{4}. \quad (3)$$

The sensitivity of multi-site interactions is not apparent from the connector energy values due to the following reasons – (i) each connector has contributions from adsorption energy (E_0 or C_1) and other pairwise interactions that dominate over contributions from multi-site interactions and (ii) also the contribution from a particular multi-site interaction is divided by the number of participating adatoms (see Eq. (3)), further making the sensitivity of connector energies to adatom relaxations less apparent. However, this model incorporates such relaxation effects as can be seen from the uniformly low CV scores for all relaxation schemes.

The connector model works well in the case of Cu(1 1 0), Al(1 1 0) and Al(1 0 0). It remains to be seen whether the connector model provides an adequate solution, without the need for any ad hoc patches, to the overlayer problem. Relaxation effects become prominent during energy calculations of adatoms near step edges; it is in such calculations the simple lattice–gas model runs into problems [16]. At the same time, accommodating the relaxation effects encountered in such calculations within the connector model might require the usage of connectors that account for the orientations of neighbor bonds, resulting in an undesirably large number of connectors in the model. A DFT-based study that compares these two models on a surface like Pt(1 1 1), where such lateral relaxation effects are known to complicate surface energy calculations, would shed some light on that matter.

3.4. Diffusion barriers and formation of 2D islands

Diffusion barriers for Cu adatoms on Cu(1 1 0) have been calculated using a variety of methods in the past [29,31,32] but, to our knowledge, not with a DFT-based method.[8] To this end, we calculated the diffusion barriers for the most common hops on a (1 1 0) surface (cf. Fig. 3) using the nudged elastic band (NEB) method [33,34]. We did not compute the barriers for long jumps and correlated exchange processes that are expected to occur on this surface at high temperatures ($T > 450$ K) [35] since these processes are tangential to the goals of this paper. The anisotropic bond-breaking model describes the diffusion barriers on (1 1 0) surfaces accurately; Mottet et al. computed the barriers on Cu(1 1 0) using Rosato, Guillopé and Legrand (RGL) potentials,[9] and their results showed that the barriers computed using the anisotropic bond-breaking model approximation are very close (within 25 meV) to the directly computed barriers [29]. Hence, the diffusion barriers for the most common hops are sufficient to model growth in the low temperature ($T < 300$ K) range. Also, diffusion through metastable walk [37] and leapfrog mechanisms [38,39] are not relevant on this surface because Cu(1 1 0) does not reconstruct. We used a (4 × 3 × 16) supercell sampled with a (4 × 4 × 2) *k*-point mesh. The in-channel and

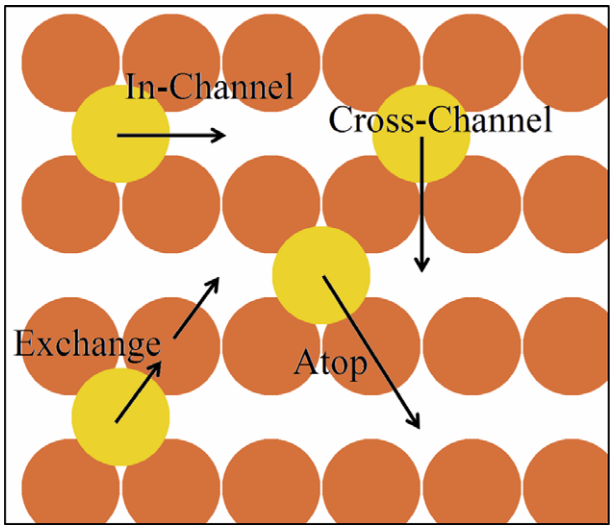

Fig. 3. Adatom hops along high-symmetry directions on a (1 1 0) surface. The corresponding barriers are given in Table 5.

[7] Adatoms with only a second-neighbor bond are mapped to C_3, while those with a second-neighbor bond along with one or more third-neighbor bonds are mapped to C_{10}.

[8] Stepanyuk et al. [32] employed VASP (PW91-GGA) to compute a few diffusion barriers for Co adatoms on Cu(110) but the barriers for diffusion of Cu adatoms were computed using molecular static (MS) calculations based on the second-moment approximation but fitted to ab-initio calculations rather than to experimental data.

[9] The attractive part of the potential is derived using the second-moment approximation to the tight-binding model and the repulsive part of the potential is assumed to be of a Born-Mayer type [36].

Table 5
Hopping barriers calculated using the NEB method. The hops are shown in Fig. 2.

Hop	Barrier (eV)
In-channel	0.322
Cross-channel	1.049
Exchange	0.351
Atop	1.448

cross-channel hopping barriers in the case of other two bigger supercells, computed by placing an adatom at the respective bridge sites, were found to be very close to the ones obtained using the $(4 \times 3 \times 16)$ supercell. Seven images were used to sample the potential energy surface.

The obtained barriers (cf. Table 5) are in good agreement with previous theoretical calculations [29,31,32]. From the computed diffusion barriers, we can say that the in-channel hopping and the exchange are the dominant mechanisms responsible for intralayer diffusion. Our in-channel hopping and exchange barriers computed using VASP (PW91-GGA) are higher than the corresponding values from second-moment methods [29,31,32]. Our in-channel diffusion barrier is 0.12 eV higher than the value computed using RGL potentials [29,31] and by about 0.06 eV higher than the value from MS calculation [32]. Similarly, the exchange barrier is about 0.05–0.1 eV higher than the values from RGL potentials and MS calculations. The reason behind the higher value of diffusion barriers in the case of VASP (PW91-GGA) is not clear. However, it should be noted that the diffusion barriers for Co on Cu(1 1 0) computed using VASP (PW91-GGA) are also higher than the corresponding values from MS calculations [32]. Even though some cross-channel interactions like E_3 and E_{T1} are repulsive, the attractive nature of E_1, E_2 and E_{C1} and the small barrier for exchange hopping lead us to expect the formation of compact 2D islands. In their kinetic Monte Carlo simulations, Mottet et al. [29] did show such formation over a suitable temperature range.

4. Conclusion

Using both the lattice–gas model and the connector model, we have quantified the interactions between Cu adatoms on Cu(1 1 0). In the case of lattice–gas model, we find strong multi-site interactions on this surface. As expected, some of these multi-site interactions are extremely sensitive to atomic relaxations. This study emphasizes the importance of multi-site interactions and the role of adatom relaxations in lattice–gas modeling of overlayer systems. Even though introducing higher-order multi-site interactions can evidently account for relaxation effects in the lattice–gas model, we look forward to the development of alternate models that can deal with adatom relaxations efficiently. The connector model provides a good alternative for the lattice–gas model on this surface and holds some promise as a possible alternative for characterizing adatom interactions. However, conclusive evidence has not yet been presented to show that the connector model is immune to surface relaxation effects. We invite studies in this direction.

Acknowledgements

This work was supported by the University of Maryland NSF-MRSEC, Grant DMR 05-20471, with ancillary support from the Center for Nanophysics and Advanced Materials (CNAM). Computational support for VASP calculations was provided by National Computational Science Alliance at University of Illinois, Urbana Champaign. We thank Kristen Fichthorn for useful exchanges. We are grateful to Suriyanarayanan Vaikuntanathan for help during the early stage of this project.

References

[1] L.D. Roelofs, in: R. Vanselow, R.F. Howe (Eds.), Chemistry and Physics of Solid Surfaces IV, Springer, Berlin, 1982 (Chapter 10).
[2] B.N.J. Persson, Surf. Sci. Rep. 15 (1992) 1.
[3] T.L. Einstein, in: W.N. Unertl (Ed.), Physical Structure of Solid Surfaces, Handbook of Surface Science, vol. 1, Elsevier, Amsterdam, 1996, p. 577.
[4] A. Patrykiejew, S. Sokolowski, K. Binder, Surf. Sci. Rep. 37 (2000) 207.
[5] G. Kresse, J. Hafner, Phys. Rev. B 47 (1993) R558.
[6] G. Kresse, J. Hafner, Phys. Rev. B 49 (1994) 14251.
[7] G. Kresse, J. Furthmüller, Comput. Mater. Sci. 6 (1996) 15.
[8] G. Kresse, J. Furthmüller, Phys. Rev. B 54 (1996) 11169.
[9] S.-J. Koh, G. Ehrlich, Phys. Rev. B 60 (1999) 5981.
[10] C. Stampfl, H.J. Kreuzer, S.H. Payne, H. Pfnür, M. Scheffler, Phys. Rev. Lett. 83 (1999) 2993.
[11] L. Österlund, M.Ø. Pederson, I. Stensgaard, E. Lægsgaard, F. Besenbacher, Phys. Rev. Lett. 83 (1999) 4812.
[12] C. Stampfl, Catal. Today 105 (2005) 17;
M. Borg et al., Chem. Phys. Chem. 6 (2005) 1923.
[13] T.J. Stasevich, T.L. Einstein, Phys. Rev. B 73 (2006) 115426.
[14] Y. Zhang, V. Blum, K. Reuter, Phys. Rev. B 75 (2007) 235406.
[15] Y. Tiwary, K.A. Fichthorn, Phys. Rev. B 75 (2007) 235451.
[16] R. Sathiyanarayanan, T.J. Stasevich, T.L. Einstein, Surf. Sci. 602 (2008) 1243.
[17] Y. Tiwary, K.A. Fichthorn, Phys. Rev. B. 78 (2008) 205418.
[18] F.B. de Mongeot, W. Zhu, A. Molle, R. Buzio, C. Boragno, U. Valbusa, E.G. Wang, Z.Y. Zhang, Phys. Rev. Lett. 91 (2003) 016102.
[19] W. Zhu, F.B. de Mongeot, U. Valbusa, E.G. Wang, Z.Y. Zhang, Phys. Rev. Lett. 92 (2004) 106102.
[20] H. Yang, Q. Sun, Z. Zhang, Y. Jia, Phys. Rev. B 76 (2007) 115417.
[21] C.C. Perry, S. Haq, B.G. Frederick, N.V. Richardson, Surf. Sci. 409 (1998) 512.
[22] S.S.P. Parkin, Z.G. Li, D.J. Smith, Appl. Phys. Lett. 58 (1991) 2710.
[23] P. Hohenberg, W. Kohn, Phys. Rev. 136 (1964) B864.
[24] W. Kohn, L. Sham, Phys. Rev. 140 (1965) A1133.
[25] J.P. Perdew, in: P. Ziesche, H. Eschrig (Eds.), Electronic Structure Theory of Solids, Akademie Verlag, Berlin, 1991;
J.P. Perdew, J.A. Chevary, S.H. Vosko, K.A. Jackson, M.R. Pederson, D.J. Singh, C. Fiolhais, Phys. Rev. B 46 (1992) 6671.
[26] M. Methfessel, A.T. Paxton, Phys. Rev. B 40 (1989) 3616.
[27] Y. Shu, J.-M. Zhang, K.-W. Xu, V. Ji, Solid State Commun. 141 (2007) 384 (and references therein).
[28] J. Shao, J. Am. Stat. Assoc. 88 (422) (1993) 486.
[29] C. Mottet, R. Ferrando, F. Hontinfinde, A.C. Levi, Surf. Sci. 417 (1998) 220 (and references therein).
[30] T.L. Einstein, Langmuir 7 (1991) 2520.
[31] U.T. Ndongmouo, F. Hontinfinde, Surf. Sci. 571 (2004) 89 (and references therein, especially for EAM calculations).
[32] O. Stepanyuk, N.N. Negulyaev, A.M. Saletsky, W. Hergert, Phys. Rev. B 78 (2008) 113406.
[33] G. Mills, H. Jónsson, G.K. Schenter, Surf. Sci. 324 (1995) 305.
[34] H. Jónsson, G. Mills, K.W. Jacobsen, in: B.J. Berne, G. Ciccotti, D.F. Coker (Eds.), Classical and Quantum Dynamics in Condensed Phase Simulations, World Scientific, 1998.
[35] F. Montalenti, R. Ferrando, Phys. Rev. B 59 (1999) 5881.
[36] V. Rosato, M. Guillopé, B. Legrand, Philos. Mag. A 59 (1989) 321.
[37] F. Montalenti, R. Ferrando, Phys. Rev. B 58 (1998) 3617.
[38] T.R. Linderoth, S. Horch, L. Petersen, S. Helveg, E. Lægsgaard, I. Stensgaard, F. Besenbacher, Phys. Rev. Lett. 82 (1999) 1494.
[39] F. Montalenti, R. Ferrando, Phys. Rev. Lett. 82 (1999) 1498.